


Eigenfunctions of Underspread Linear Communication Systems

Sergio Barbarossa and Mikhail Tsitsvero

October 14, 2015

1 Introduction

he knowledge of the eigenfunctions of a linear time-varying (LTV) system is a fundamental issue from both theoretical and applications points of view. Nonetheless, no analytic expressions are available for the eigenfunctions of a general LTV system. However, approximate expressions have been proposed for slowly-varying operators. In particular, in [1] it was shown that an underspread system can be well approximated by a normal operator, so that we can properly talk about eigendecomposition. The interesting result derived in [1] is that the class of eigenfunctions of underspread systems can be approximated by a set of signals obtained as shifted versions, in both time and frequency, of a given pulse waveform $g(t)$, which is well localized in the time-frequency domain. The validity of this approximation depends on the system spread along the delay and Doppler axes. An alternative approach, for Hermitian slowly-varying operators, was proposed in [4], [5] and [6] where the authors used the WKB (Wentzel-Kromers-Brillouin) method to derive a relationship between the instantaneous frequency of the channel eigenfunctions and the contour lines of the Wigner Transform of the operator kernel (or Weyl symbol).

In this paper, we will follow an approach similar to [4] and show that the eigenfunctions can be found exactly for systems whose delay-Doppler spread function is concentrated along a straight line and they can be found in approximate sense for systems having a spread function maximally concentrated in regions of the Doppler-delay plane whose area is smaller than one. The interesting results are that: i) the instantaneous frequency of the eigenfunctions is dictated by the contour level of the time-varying transfer function; ii) the eigenvalues are restricted between the minimum and maximum value of the the system time-varying transfer functions, but not all values are possible, as the system exhibits an inherent quantization.

⁰Authors: **Sergio Barbarossa** and **Mikhail Tsitsvero**, Department of Information Engineering, Electronics and Telecommunications, University of Rome “La Sapienza”, Via Eudossiana 18, 00184 Rome, Italy (sergio.barbarossa@uniroma1.it, tsitsvero@gmail.com).

2 Channel Characterizations

We will consider input/output relationship for a continuous-time LTV system $y(t) = (\mathbf{H}x)(t)$. This relationship may be represented as following¹

$$y(t) = (\mathbf{H}x)(t) = \int h(t, \tau)x(t - \tau) d\tau = \int k(t, \tau)x(\tau) d\tau, \quad (1)$$

where $h(t, \tau)$ is the channel response at time t to an impulse sent at time $t - \tau$, while $k(t, \tau)$ is the channel response at time t to an impulse sent at time τ . We will refer to $h(t, \tau)$ as *time-varying impulse response* and to $k(t, \tau)$ as *time-varying impulse response kernel* [7]. Any linear time-varying channel may be equivalently characterized by the *delay-Doppler spreading function* $S(\tau, \nu)$

$$S(\tau, \nu) = \int h(t, \tau)e^{-j2\pi\nu t} dt \quad (2)$$

or by the *time-varying transfer function* $H(t, f)$

$$H(t, f) = \int h(t, \tau)e^{-j2\pi f\tau} d\tau. \quad (3)$$

The corresponding adjoint channel is denoted as \mathbf{H}^* and it corresponds to the following input/output relation

$$y(\tau) = (\mathbf{H}^*x)(\tau) = \int h^*(t, t - \tau)x(t) dt. \quad (4)$$

3 Channel Decomposition

In general, LTV systems are not Hermitian (i.e. $\mathbf{H} \neq \mathbf{H}^*$), so that they may not admit the canonical eigendecomposition over a set of orthonormal eigenfunctions with real-valued eigenvalues. However, they may be properly characterized by introducing the *left and right singular functions* with corresponding *real-valued singular values*.

Definition 3.1 *The functions $u_i(t)$, $v_i(t)$ are the left and right singular functions of the system \mathbf{H} with a corresponding singular value $\sigma_i \in \mathbb{R}^+$ if the following relationships are satisfied*

$$\sigma_i u_i(t) = (\mathbf{H}v_i)(t), \quad (5)$$

$$\sigma_i v_i(t) = (\mathbf{H}^*u_i)(t). \quad (6)$$

From these expressions it is clear that left and right singular functions are the eigenfunctions of the composite Hermitian systems $\mathbf{H}\mathbf{H}^*$ and $\mathbf{H}^*\mathbf{H}$, respectively, with corresponding eigenvalues equal to σ_i^2 .

If the system impulse response is square-integrable, i.e.

$$\int \int |h(t, \tau)|^2 dt d\tau < \infty, \quad (7)$$

¹Limits of integration are assumed to be from $-\infty$ to ∞ if not explicitly specified

then there exists [8] a sequence (finite or infinite) of positive decreasing numbers $\sigma_1 \geq \dots \geq \sigma_i \geq \dots > 0$, which are the singular values of this system, and two sets of corresponding orthonormal left and right singular functions $u_i(t)$ and $v_i(t)$.

However, it is worth noting that there are at least a few important cases for which $h(t, \tau)$ is not square integrable, as for example in linear time-invariant (LTI) or linear frequency invariant (LFI) channels, i.e. when $h(t, \tau)$ is constant along t or when $h(t, \tau) = m(t)\delta(\tau)$.

4 Exact and Approximate Solutions

4.1 Spreading Function Concentrated over a Straight Line

Let us start considering a channel having spreading function $S(\nu, \tau)$ with support concentrated solely over a straight line on the (ν, τ) -plane, i.e. $S(\nu, \tau) = g(\tau)\delta(\nu - \mu\tau - f_0)$. A practical example of this class could be a multipath channel with two paths. Using (2), the time-varying impulse response of such system is:

$$h(t, \tau) = g(\tau)e^{j2\pi\mu\tau t}e^{j2\pi f_0 t}. \quad (8)$$

In this case, the singular functions can be expressed in closed form, as stated next.

Theorem 4.1 *Let us consider a system \mathbf{H} with spreading function $S(\nu, \tau) = g(\tau)\delta(\nu - \mu\tau - f_0)$, where μ and f_0 are real parameters and $g(\tau)$ is a smooth function. Then the left and right singular functions and singular values of this system are*

$$v_i(t) = e^{j2\pi f_i t}e^{j\pi\mu t^2}, \quad (9)$$

$$u_i(t) = e^{j2\pi f_0 t}e^{j\arg K(f_i, \mu)}v_i(t), \quad (10)$$

$$\sigma_i = |K(f_i, \mu)|, \quad (11)$$

where $K(f_i, \mu) = \int g(\tau)e^{-j2\pi f_i \tau}e^{j\pi\mu\tau^2} d\tau$.

The proof may be obtained by direct substitution of (8) into (1).

Remark 1 *From (3), the time-varying transfer function of the system in (8) is*

$$H(t, f) = e^{j2\pi f_0 t}G(f - \mu t). \quad (12)$$

At the same time, the instantaneous frequencies of the left and right singular functions are, respectively, $f^l(t) = f_i + \mu t$ and $f^r(t) = f_0 + f_i + \mu t$. Hence, combining this result with (12), we can draw the conclusion that the instantaneous frequencies of the left and right singular functions correspond to regions in the time-frequency plane where the time-varying transfer function is constant.

4.2 Spreading Function with Limited Support

Let us consider now the case where the spreading function is mainly concentrated over a limited support in the delay-Doppler domain. If we consider the composite systems $\mathbf{H}\mathbf{H}^*$, we can write

$$\sigma_i^2 u_i(t) = \int \mathcal{K}(t, \theta) u_i(\theta) d\theta, \quad (13)$$

where the kernel $\mathcal{K}(t, \theta)$ is defined as

$$\mathcal{K}(t, \theta) = \int h(t, t - \tau) h^*(\theta, \theta - \tau) d\tau. \quad (14)$$

In this case, it is not possible to express the singular functions in closed form. Nevertheless, using the WKB method, as shown in the Appendix, we can still provide an approximated closed form solution:

$$u_i(t) = \sum_m A_{i,m}(t) e^{j\phi_{i,m}(t)}, \quad (15)$$

$$\left| H\left(t, \frac{\dot{\phi}_{i,m}(t)}{2\pi}\right) \right|^2 = \sigma_i^2, \quad (16)$$

$$A_{i,m}(t) = \left[\left| \frac{\partial |H(t, f)|^2}{\partial f} \right| \right]^{-1/2} \bigg|_{f=\frac{\dot{\phi}_{i,m}(t)}{2\pi}}. \quad (17)$$

Remark 2 *The instantaneous frequency of each component of the left singular function is still given, as in the previous section, by the curves in the time-frequency plane where the time-varying transfer function is constant. Furthermore, the instantaneous bandwidth of each component depends on the derivative of the time-varying transfer function evaluated along the instantaneous frequency curves².*

Remark 3 *From (17), the amplitude $A_{i,m}(t)$ diverges at points where the partial derivative is zero. These points are denoted as **turning points**, in analogy with what appears in the WKB solution of Schroedinger equation in physics. In the neighbourhood of these points, the solution (16) and (17) is no longer valid and the problem must be analyzed separately.*

4.3 Area Rule

From (16) it appears that the singular values are bounded between the minimum and maximum values of $|H(t, f)|$. However, it is still unclear if the singular values may assume any value within this interval. The answer is: no. It turns out that, under the square integrability assumption (7), the contour lines of $|H(t, f)|$ surface are always represented by a set of closed curves. In the following, we will refer to these closed curves as to *bubbles* in time-frequency domain. A pictorial example of a bubble (contour plot of $|H(t, f)|$) is shown in Fig. 1. Each bubble has an even number of turning points. Moreover, without any loss of generality, we will associate to each bubble its own eigenfunction $u_i(t)$ with a number of components in the sum (15) equal to the number of turning points. What happens is that the only admissible values of σ_i are the ones satisfying the so called *area rule*, stating that the area of the bubble associated to the level σ_i must be equal to $n_i + 1/2$, where n_i is an integer nonnegative number.

This condition is known in physics as EBK (Einstein-Brillouin-Keller) quantization formula (see [5]). In our context, it gives a natural criterion for choosing

²The instantaneous bandwidth was defined in [16] as $B(t) = |A'(t)/A(t)|$

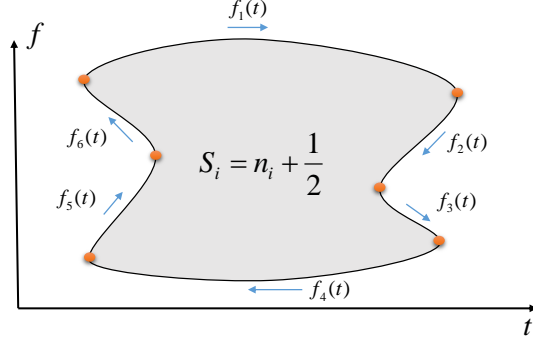


Figure 1: Example of a bubble with six turning points

the right values of σ_i . It is also worth to note here that the phase increments by $\pi/2$ at convex turning points and decrements by $\pi/2$ at concave turning points [5] for the traversing of the bubble as it is shown in Fig. 1.

5 Numerical Validation

In deriving analytic expressions for the singular functions we used approximations whose validity limits need to be checked. Since the analytic models have a very specific structure in the time-frequency domain, the natural tool to analyze the results is a time-frequency representations with good time-frequency localization capabilities. To this purpose, we use here the smoothed pseudo Wigner-Ville distribution (SPWVD) with a reassignment procedure, as developed by [9] and [10].

5.1 Experimental Setup

We consider a channel with band limited input and time limited output, which may be approximately described as a windowing of time-varying transfer function $H(t, f)$ in both time and frequency. This leads to a square-integrable time-varying impulse response $h(t, \tau)$.

By assuming input signal $x(t)$ to be bandlimited within the interval $[-1/2T_s, 1/2T_s]$ we can express it in accordance with the sampling theorem

$$x(t) = \sum_k x[k] \text{sinc} \left(\frac{t - kT_s}{T_s} \right), \quad (18)$$

where $\text{sinc}(x) := \sin(\pi x)/\pi x$, $x[k] := x(kT_s)$ and T_s is a sampling time. By sampling the continuous time output $y(t)$ with same sampling rate $1/T_s$, we obtain the equivalent discrete-time input-output relationship

$$y[n] = \sum_k h[n, n - k] x[k], \quad (19)$$

where $y[n] := y(nT_s)$ and $h[n, k]$ is the equivalent discrete time time-varying impulse response defined by

$$h[n, n - k] := \int \int h(\theta, \tau) \text{sinc} \left(\frac{nT_s - \theta}{T_s} \right) \text{sinc} \left(\frac{\theta - \tau - kT_s}{T_s} \right) d\tau d\theta. \quad (20)$$

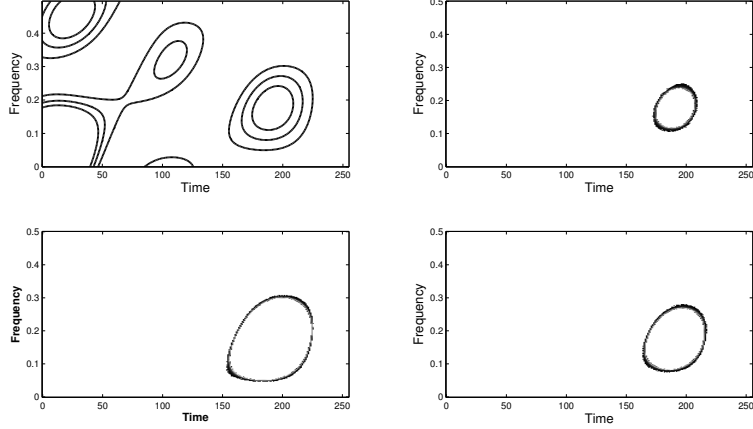


Figure 2: Contour lines of $|H(t, f)|$ for the multipath case corresponding to three different levels (left top) and time-frequency distributions of singular vectors \mathbf{u}_{25} (top right), \mathbf{u}_{40} (bottom right) and \mathbf{u}_{72} (bottom left)

Using (20) the discrete-time counterpart of (1) may be rewritten as

$$\mathbf{y} = \mathbf{H}\mathbf{x}, \quad (21)$$

where \mathbf{H} is the channel matrix. The left and right singular vectors \mathbf{u}_i , \mathbf{v}_i of \mathbf{H} can be obtained by computing the singular value decomposition (SVD) of \mathbf{H}

$$\mathbf{H} = \mathbf{U}\mathbf{\Sigma}\mathbf{V}^*, \quad (22)$$

where the columns of \mathbf{U} and \mathbf{V} are the left and right singular vectors \mathbf{u}_i , \mathbf{v}_i associated to the singular value σ_i contained in the diagonal matrix $\mathbf{\Sigma}$.

We check the validity of our theoretical expressions through the following steps: 1) build the channel matrix \mathbf{H} ; 2) compute the SVD of \mathbf{H} ; 3) compute the reassigned SPWVD (RSPWVD) of the singular vectors associated to some singular value σ_i , [9]; 4) compare the results obtained from (16) and (17) with singular vectors computed numerically.

As we consider a windowed version of time-varying transfer function $H(t, f)$ the application of the area rule in some cases may not be straightforward because it is possible that the bubbles will be broken on the edges of the window. In these situations we observed an interesting feature that the area rule still holds exactly, however one should encounter just parts of the bubbles limited by the edges of the window.

5.2 Multipath Case

As a test example, we consider a multipath channel with time-varying impulse response of the form

$$h(t, \tau) = \sum_{q=0}^{Q-1} h_q e^{j2\pi f_q t} \delta(\tau - \tau_q), \quad (23)$$

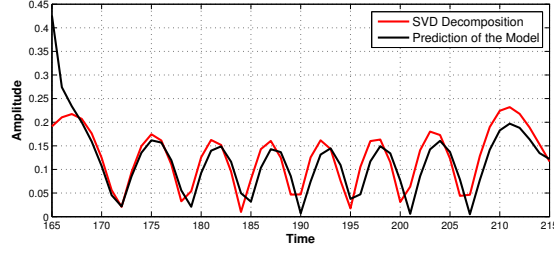


Figure 3: Comparison of the amplitude of \mathbf{u}_{40} with one, predicted by the model

where each of the Q paths is attenuated by h_q , delayed in time by τ_q and Doppler shifted by f_q . In accordance with Rayleigh fading model, we model h_q as independent identically distributed (i.i.d.) complex Gaussian random variables having zero mean and unit variance. Time shifts τ_q and Doppler shifts f_q are modeled as uniformly i.i.d. random variables within intervals $[0, \Delta\tau]$ and $[-\Delta f/2, \Delta f/2]$ respectively. In such a case, from (3), the time-varying transfer function is

$$H(t, f) = \sum_{q=0}^{Q-1} h_q e^{j2\pi f_q t} e^{-j2\pi \tau_q f}. \quad (24)$$

We provide the results of simulation for $Q = 10$ path channel, with $\Delta\tau = 4T_s$ and $\Delta f = 4/NT_s$, $N = 256$. In Fig. 2 three contour levels (corresponding to σ_{25} , σ_{40} and σ_{72}) of $|H(t, f)|$ are given alongside with the time-frequency distributions (RSPWVD) of the corresponding singular vectors. We can observe a very good agreement between the numerical results and the behaviors predicted by the proposed analytic models. Next we compare the amplitudes for numerically calculated singular vectors \mathbf{u}_{40} with singular functions obtained by applying the formula (17). The result is shown in Fig. 3. One can note a slight departure between theoretical models and numerical results, essentially due to small errors around the turning points that accumulate in the computation of the instantaneous phase from its derivative using discrete integration methods (simple trapezium method).

As a further illustration of the nested structure of the bubbles in time-frequency domain, we consider the prolate spheroidal functions, known to be the singular functions of the system approximately limited both in time and frequency (see [13], [14] and [15] for details). In Fig. 4 we report the contour plots of the RSPWVD of three prolate spheroidal sequences corresponding to three different singular values (decreasing - from top to bottom) of a given time and bandwidth limiting operators. It is interesting to observe how these waveforms fill the time-frequency region while being nested within each other rather than filling the same space through the usual rectangular tiling.

6 Optimal Waveforms for Digital Communications through LTV Channels

One motivating application of the theory described above is digital communication through an LTV channel. In Article 13.2, for example, it is shown how

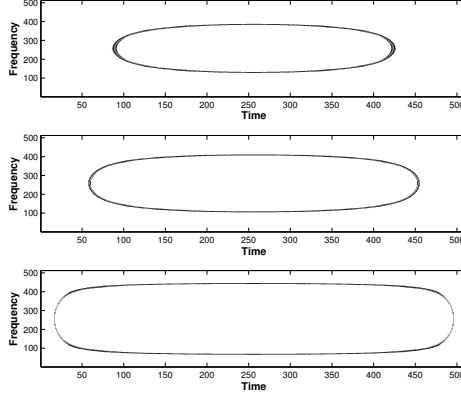


Figure 4: Time-frequency distributions of prolate spheroidal functions

to convert the channel dispersiveness, possibly in both time and frequency domains, into a useful source of diversity to be exploited to enhance the SNR at the receiver. Here we show that if the transmitter is able to predict the channel time-varying transfer function, at least within the next time slot where it is going to transmit, it is possible to optimize the transmission strategy and take full advantage of the diversity offered by the channel dispersiveness (see e.g. [12] for more details).

Considering a channel with approximately finite impulse response of order L , we can parse the input sequence in consecutive blocks of K symbols and insert null guard intervals of length L between successive blocks to avoid inter-block interference. If the symbol rate is $1/T_s$, the time necessary to transmit each block is KT_s . For each i -th block, we must consider the channel $h_i(t, \tau)$ obtained by windowing $h(t, \tau)$ in time, in order to retain only the interval $[iKT_s, (i+1)KT_s]$, and in frequency, keeping only the band $[-1/2T_s, 1/2T_s]$. The optimal strategy for transmitting a set of symbols $s_i[k] := s[iK+k]$, $k = 0, \dots, K-1$, in the presence of additive white Gaussian noise (AWGN), is to send the signal [8, sec. 8]

$$x_i(t) = \sum_{k=0}^{K-1} c_{i,k} s_i[k] v_{i,k}(t) \quad (25)$$

where $v_{i,k}(t)$ is the right singular function associated to the k -th eigenvalue of the channel response $h_i(t, \tau)$ in the i -th transmit interval and $c_{i,k}$ are coefficients used to allocate the available power among the transmitted symbols according to some optimization criterion [12]. Using (5) and (6), the received signal is thus

$$y_i(t) = \int_{-\infty}^{\infty} h_i(t, \tau) x_i(t - \tau) d\tau + w(t) = \sum_k c_{i,k} \sigma_{i,k} s_i[k] u_{i,k}(t) + w(t), \quad (26)$$

where $u_{i,k}(t)$ is the left singular function associated to the k -th singular value of $h_i(t, \tau)$ and $w(t)$ is AWGN. Hence, by exploiting the orthonormality of the functions $u_{i,k}(t)$, the transmitted symbols can be estimated by simply taking the scalar products of $y(t)$ with the left singular functions, i.e.

$$\hat{s}_i[m] = \frac{1}{\sigma_{i,m} c_{i,m}} \int_{-\infty}^{\infty} y(t) u_{i,m}^*(t) dt = s_i[m] + w_i[m], \quad (27)$$

where the noise samples sequence $w_i[m] := \int_{-\infty}^{\infty} w(t) u_{i,m}^*(t) dt$ constitutes a sequence of i.i.d. Gaussian random variables. In this way, the initial LTV channel, possibly dispersive in both time and frequency domains, has been converted into a set of parallel independent non-dispersive subchannels, with no intersymbol interference, and the symbol-by-symbol decision is also the maximum likelihood detector.

Most current transmission schemes turn out to be simple examples of the general framework illustrated in this paper. For example, in communications through flat fading multiplicative channels, whose eigenfunctions are Dirac pulses, hence the optimal strategy is time division multiplexing. By duality, the optimal strategy for linear time-invariant channels is orthogonal frequency division multiplexing (OFDM). In the most general case (of underspread channels), the optimal strategy would consist in sending symbols through channel-dependent waveforms that fill the assigned time-frequency frame according to the nested bubble-like structures illustrated in this paper. Of course, the limit of validity of such an approach is dictated by the capability to provide a sufficiently accurate short term prediction of the channel variation, based on past observations.

7 Summary and Conclusions

The analytic model for the eigenfunctions of underspread linear operators shown in this article, although approximate, shows that the energy of the system eigenfunctions is mainly concentrated along curves coinciding with level curves of the system transfer function. Numerical results show that indeed the analytic model fits very well with the numerical results. This model provides a general framework for interpreting some current data transmission schemes and, most importantly, gives a new perspective on the selection of the optimal waveforms to be used for transmissions over time-varying channels.

8 Appendix

To facilitate the analysis of slowly varying systems, the kernel $\mathcal{K}(t, \theta)$ may be rewritten in terms of the difference $t - \theta$ and the mean $(t + \theta)/2$ as:

$$\mathcal{K}(t, \theta) = K \left(t - \theta, \frac{\epsilon}{2}(t + \theta) \right), \quad (28)$$

where $\epsilon \ll 1$ is a parameter representing the small dependence on $(t + \theta)/2$ (a time invariant system simply corresponds to $\epsilon = 0$). This formulation suggests [4], [5] the following form for the solution of (13)

$$u_i(t; \epsilon) = \sum_k A_{i,k}(\epsilon t; \epsilon) e^{j\phi_{i,k}(\epsilon t; \epsilon)/\epsilon}. \quad (29)$$

To clarify the meaning of (28) and (29) let us consider the following Taylor series expansion of the amplitude and phase in (29) around an arbitrary point

$$t = t_0$$

$$u_i(t; \epsilon) = e^{j \sum_{n=0}^{\infty} (-1)^n \epsilon^{n-1} (t-t_0)^n \phi_i^{(n)}(\epsilon t_0)/n!} \cdot \sum_{n=0}^{\infty} (-1)^n \epsilon^n A_i^{(n)}(\epsilon t_0) (t-t_0)^n / n!. \quad (30)$$

From (30) it becomes clear that solution of the form (29) allows us to expand (29) in power series of ϵ , by taking different orders for the phase and the amplitude.

Solutions of the form (29) are usually called WKB (Wentzel-Kromers-Brillouin) solutions and the associated method of finding approximate solutions is usually applied to differential operators, however [5] proved it to be very well applicable to the wide class of integral operators. What we consider here is just a particular case of the well developed perturbation theory.

Here and thereafter we assume that all series expansions in ϵ converge, however it may not always be the case and it is subject to additional analysis and corrections. Now, if we put $\epsilon \approx 0$, we immediately come to the “unperturbed” solution in the form of approximate complex exponentials with constant amplitude. The “unperturbed” kernel (28) will depend only on the difference $t - \theta$, therefore this case is generally equivalent to the case of LTI systems. On the other hand, $\epsilon = 1$ leads to the true solution of (13). So the solution is first examined by using power series of small parameter ϵ and then these results are extended to the solution of (13).

By making a change of variables $q = \epsilon t$ and $u = t - \theta$ in (28) and considering for simplicity (and without loss of generality) only a single term in the sum of (29), we can rewrite (13) as

$$\sigma_i^2 A_{i,m}(q; \epsilon) = \int K(u, q - \epsilon u/2) A_{i,m}(q - \epsilon u; \epsilon) \cdot e^{j(\phi_{i,m}(q - \epsilon u) - \phi_{i,m}(q))/\epsilon} du. \quad (31)$$

By taking the limit $\epsilon \rightarrow 0$, we come to

$$\int K(u, q) e^{-ju\dot{\phi}_{i,m}(q)} du = \sigma_i^2. \quad (32)$$

Or, alternatively, by introducing the function $\tilde{K}(p, q)$

$$\tilde{K}(p, q) = \int K(u, q) e^{-j2\pi up} du, \quad (33)$$

which is also referred to as Wigner transform of $K(u, q)$ [5], we can rewrite (32) as

$$\tilde{K}\left(\frac{\dot{\phi}_{i,m}(q)}{2\pi}, q\right) = \sigma_i^2. \quad (34)$$

This is an implicit equation showing that the instantaneous phase $\phi_{i,m}(q)$ must be chosen such that condition (34) is satisfied. Operator $\mathbf{H}\mathbf{H}^*$ is hermitian by definition, therefore $\tilde{K}(p, q)$ is real.

Now after making Taylor series expansion of each term in (31) around $\epsilon = 0$

we can write, taking into account (32) and considering only terms $\propto \epsilon$,

$$\int \left[\frac{u}{2} \frac{\partial K(u, q)}{\partial q} A_{i,m}(q) + u K(u, q) \frac{dA_{i,m}(q)}{dq} - j A_{i,m}(q) K(u, q) \frac{u^2}{2} \frac{d^2 \phi_{i,m}(q)}{dq^2} \right] e^{-ju\phi_{i,m}(q)} du = 0. \quad (35)$$

Equation (35) may be thought as condition to null the term proportional to ϵ in expansion of (31).

For further simplicity of notation we introduce the functions $\tilde{K}_{i,j}(p, q)$ as

$$\tilde{K}_{i,j}(p, q) = \frac{\partial^{i+j} \tilde{K}(p, q)}{\partial p^i \partial q^j}. \quad (36)$$

By noticing that

$$\begin{aligned} j \tilde{K}_{1,1} \left(\frac{\dot{\phi}_{i,m}(q)}{2\pi}, q \right) &= 2\pi \int u \frac{\partial K(u, q)}{\partial q} e^{-ju\phi_{i,m}(q)} du \\ - j 2\pi \frac{d^2 \phi_{i,m}(q)}{dq^2} \int u^2 K(u, q) e^{-ju\phi_{i,m}(q)} du \end{aligned} \quad (37)$$

we can restate (35) as

$$\frac{d}{dq} \left[A_{i,m}^2(q) \tilde{K}_{1,0} \left(\frac{\dot{\phi}_{i,m}(q)}{2\pi}, q \right) \right] = 0. \quad (38)$$

This equation shows that the amplitude must be a solution of (38).

As a next step we establish the relationship between function $\tilde{K}(p, q)$ and time-varying transfer function $H(t, f)$. It would be useful to represent $\tilde{K}(p, q)$ in terms of time-varying impulse response $h(t, \tau)$. Combining (14), (28) and (33) we can easily see that

$$\tilde{K}(p, q) = \int \int h \left(\frac{u}{2} + \frac{q}{\epsilon}, \frac{u}{2} + \frac{q}{\epsilon} - \tau \right) h^* \left(-\frac{u}{2} + \frac{q}{\epsilon}, -\frac{u}{2} + \frac{q}{\epsilon} - \tau \right) e^{-jup} du d\tau. \quad (39)$$

And by exploiting the fact that $h(t, \tau)$ is the inverse Fourier transform of $H(t, f)$ with respect to f , we obtain

$$\tilde{K}(p, q) = \int \int H \left(\frac{u}{2} + \frac{q}{\epsilon}, \nu \right) \cdot H^* \left(-\frac{u}{2} + \frac{q}{\epsilon}, \nu \right) e^{-j2\pi(p-\nu)u} du d\nu. \quad (40)$$

Following the spirit of the previous discussion we try to find the equation of the curve where $\tilde{K}(p, q)$ is constant. By denoting for simplicity $p(q) = \dot{\phi}_{i,m}(q)/2\pi$ and assuming that $H(\pm \frac{u}{2} + \frac{q}{\epsilon}, \nu) \approx H(\frac{q}{\epsilon}, \nu)$ we can rewrite $\tilde{K}(p(q), q)$ as

$$\tilde{K}(p(q), q) \approx \int \left| H \left(\frac{q}{\epsilon}, \nu \right) \right|^2 \int e^{-j2\pi(p(q)-\nu)u} du d\nu = \left| H \left(\frac{q}{\epsilon}, p(q) \right) \right|^2. \quad (41)$$

Therefore, putting $\epsilon = 1$, we can write instead of (29), (34) and (38)

$$u_i(t) = \sum_m A_{i,m}(t) e^{j\phi_{i,m}(t)}, \quad (42)$$

$$\left| H\left(t, \frac{\dot{\phi}_{i,m}(t)}{2\pi}\right) \right|^2 = \sigma_i^2, \quad (43)$$

$$A_{i,m}(t) = \left[\left| \frac{\partial |H(t, f)|^2}{\partial f} \right| \right]^{-1/2} \bigg|_{f=\frac{\dot{\phi}_{i,m}(t)}{2\pi}}. \quad (44)$$

References

- [1] G. Matz and F. Hlawatsch, “Time-frequency transfer function calculus (symbolic calculus) of linear time-varying systems (linear operators) based on a generalized underspread theory,” *J. of Mathematical Physics*, vol. 39, pp. 4041–4070, August 1998. Special Issue on Wavelet and Time-Frequency Analysis.
- [2] Franz Hlawatsch and Gerald Matz, Eds., *Wireless Communications Over Rapidly Time-Varying Channels*, Academic Press, 2011.
- [3] G. Matz, H. Boelcskei and F. Hlawatsch, Time-frequency foundations of communications, *IEEE Signal Processing Magazine*, Vol. 30, No. 6, pp. 87-96, Nov. 2013.
- [4] L. Sirovich and B. W. Knight, “On the eigentheory of operators which exhibit a slow variation,” *Quarterly of Applied Mathematics*, vol. 38, pp. 469–488, 1980.
- [5] B.W. Knight, L. Sirovich, The eigenfunction problem in higher dimensions: Asymptotic theory, *Proc. Nati. Acad. Sci. USA*, Vol. 82, pp. 8275-8278, December 1985, Applied Mathematical Sciences
- [6] B.W. Knight, L. Sirovich, The eigenfunction problem in higher dimensions: Exact results, *Proc. Nati. Acad. Sci. USA*, Vol. 83, pp. 527-530, February 1986, Applied Mathematical Sciences.
- [7] P. A. Bello, “Characterization of randomly time-variant linear channels,” *IEEE Trans. Communication Systems*, vol. 11, pp. 360–393, December 1963.
- [8] R. G. Gallager, *Information Theory and Reliable Communication*. New York: Wiley, 1968.
- [9] F. Auger, P. Flandrin, Yu-Ting Lin, S. McLaughlin, S. Meignen, T. Oberlin, Hau-Tieng Wu, Time-Frequency Reassignment and Synchrosqueezing: An Overview, *Signal Processing Magazine, IEEE* (Volume:30 , Issue: 6), 2013.
- [10] F. Auger, O. Lemoine, P. Goncalves and P. Flandrin, *The Time-Frequency Toolbox*, available at <http://tftb.nongnu.org/>.
- [11] F. Auger and P. Flandrin, “Improving the readability of time-frequency and time-scale representations by the reassignment method,” *IEEE Trans. Signal Processing*, vol. 43, pp. 1068–1089, May 1995.

- [12] S. Barbarossa and A. Scaglione, "Time-varying fading channels," in *Signal Processing Advances in Wireless and Mobile Communications* (G. B. Giannakis, Y. Hua, P. Stoica, and L. Tong, eds.), vol. 2: "Trends in Single- and Multi-User Systems", ch. 1, Upper Saddle River, NJ: Prentice-Hall, 2001.
- [13] D. Slepian and H. O. Pollak, Spheroidal wave functions, Fourier analysis, and uncertainty—I, *Bell Syst. Tech. J.*, vol. 40, no. 1, pp. 43-63, 1961.
- [14] H. J. Landau and H. O. Pollak, Prolate spheroidal wave functions, Fourier analysis and uncertainty—II, *Bell Syst. Tech. J.*, vol. 40, no. 1, pp. 65-84, 1960.
- [15] H. J. Landau and H. O. Pollak, Prolate spheroidal wave functions, Fourier analysis and uncertainty—III: The dimension of the space of essentially time- and band-limited signals, *Bell Syst. Tech. J.*, vol. 41, pp. 1295-1336, 1962.
- [16] L. Cohen, C. Lee, "Instantaneous Bandwidth for Signals and Spectrogram," *Proc. of ICASSP 1990*, pp. 2451-2454, Apr. 1990.